Journal of Thermal Analysis and Calorimetry, Vol. 95 (2009) 1, 293–303

A NEW APPROACH FOR ISOTHERMAL CALORIMETRIC TECHNIQUE

*H. Hojjati and S. Rohani**

Department of Chemical and Biochemical Engineering, 1151 Richmond St. North, The University of Western Ontario
London, Ontario, N6A 5B9, Canada

Using flexible heat flux sensors mounted on the lateral and bottom of outside reactor wall, a new approach is developed for isothermal calorimetric technique to overcome the disadvantages of heat flow calorimetric methods. Although the proposed system needs a calibration procedure before or after the reaction completion to evaluate the lateral heat transfer area, the measurement is versatile and totally independent of the reaction media, jacket fluid, and the variations of heat transfer coefficient. Knowledge of the variations of the heat transfer coefficient is essential for the effective control and scale up of a reactor and can be inferred by the new method during the reaction. The stirrer power and the heat loss can be determined easily as well. No pre-calibration is needed for the sensors and no heating element is applied inside the reactor for temperature control. Experiments are carried out to validate the performance of the new proposed technique. With the help of a heater, the heat generated in the reactor is measured at various levels of power input. The predicted heater power inputs are in good agreement with the corresponding heat inputs. The relative detection limit in the range of 0.8–1 W L^{-1} is expected for this technique. Using the hydrolysis of acetic anhydride, the heat of reaction at 25°C is determined, which is within the range reported in the literatures. The capability of the system to deal with the variations in the overall heat transfer coefficient is also demonstrated using a simulated reaction.

Keywords: *acetic anhydride, calorimetry, detection limit, heat flux sensor, isothermal heat-flow, overall heat transfer coefficient, reaction calorimetry, semi-batch reactor*

Introduction

The main goal of reaction calorimetry is to measure the heat effects of physical and chemical changes during a process and then to relate the effects to appropriate properties such as conversion of a reaction. The approach is relatively simple, non-invasive, non-destructive, rapid and robust. It is based on the conservation equations of mass and energy using easily measurable physical data such as temperature and flow. Representing the molar enthalpy of reaction, the total heat generated or consumed by a reaction is measured and then related to the thermodynamic data, the conversion and the kinetic data of a reaction. Determination of kinetic parameters (activation energy and pre-exponential factor) [1–3], conversion of the reaction [4–7], thermodynamic parameters (heat of reaction) [2, 3, 6, 7], optimal feed policy for the semi-batch reactor under safe condition [6, 7], and heat transfer coefficient of the reactor content [3] have been reported in the literature using the calorimetric approach. The calorimetric applications for assessment of process hazards due to exothermic reactions [1, 8–10]; for the scale-up purposes [10]; for investigation of polymerization [11–15], biological, and biochemical processes [16–19]; as well as for the study of crystallization of chemicals or pharmaceuticals [20–24] have also been published in several articles.

There are various thermal analysis devices including bomb calorimeter, differential scanning calorimetry (DSC) and thermogravimetric analysis (TG), which can be categorized in calorimetric techniques. However, the aim of this work is to focus on isothermal-heat flow reaction calorimetry.

For a typical reaction calorimeter, the heat of reaction (q_r) can be estimated using an energy balance of the form:

$$\left(\sum_i m_i c_{p,i} + \sum_k m_k c_{p,k}\right)\frac{dT_r}{dt} = (q_f + q_{hm} + q_h + q_s) - (q_{ex} + q_l) + q_r \quad (1)$$

where m_i and $c_{p,i}$ are mass and specific heat capacity of i^{th} components in the reaction media, m_k and $c_{p,k}$ are mass and specific heat capacity of k^{th} instruments (e.g. temperature sensor) or equipment (e.g. impeller) inserted inside the reactor, respectively, T_r is the reaction temperature, and t is the time.

The first term in parenthesis on the right-hand of Eq. (1) represents the cumulative rate of energy input due to reactant dosing (q_f), heat of mixing (q_{hm}), the power input by the heater (q_h) and power of the mixer (q_s). The second term represents the rate of output energy including the rate of heat transfer between the reactor content and jacket fluid (q_{ex}), and heat losses from the reactor wall to the surroundings (q_l). The last

* Author for correspondence: rohani@eng.uwo.ca

1388–6150/$20.00

Akadémiai Kiadó, Budapest, Hungary
Springer, Dordrecht, The Netherlands

term (q_r) includes the rate of all energy consumed (with negative sign) or generated (with positive sign) due to both chemical and physical changes within the reaction media.

Equation (1) can be simplified for different modes of operation such as isothermal, temperature programmed, isoperibolic, and adiabatic modes of operation. In the isothermal mode, the reactor temperature is kept constant, whereas in the temperature-programmed mode, the temperature is varied according to a predefined policy. In the isoperibolic mode, the reactor temperature is allowed to vary, but the jacket temperature is maintained constant. In adiabatic mode the heat losses from the reactor are very small [25].

For isothermal mode of reaction calorimetry, therefore, Eq. (1) is simplified to:

$$(q_f+q_{hm}+q_h+q_s)-(q_{ex}+q_l)+q_r=0 \quad (2)$$

Among different terms in energy balance equation, Eq.(2), heat exchange between the reactor content and the jacket fluid (q_{ex}) is the crucial parameter to estimate the heat effects. There are four basic methods, or combination of them [26, 27], for the evaluation of q_{ex} under isothermal operation (steady state).

Heat flow calorimetry

With heat flow calorimetry, the reactor temperature (T_r) is controlled or varied by manipulating the temperature (T_j) of the cooling/heating liquid through the jacket. Under isothermal operation, the rate of heat exchange is:

$$q_{ex}=UA(T_r-T_j) \quad (3)$$

where A is heat transfer surface and U is the overall heat transfer coefficient, which is a function of convective heat transfer coefficient on the reaction side, thermal conductivity of reactor wall, convective heat transfer coefficient on the jacket side, and reactor wall dimensions.

The temperature difference is large enough to assess and can be easily measured using high precision in situ thermocouples. The flow rate of jacket fluid has to be as high as possible to control the reaction temperature isothermally. In this case, the difference between jacket inlet ($T_{j,in}$) and outlet ($T_{j,out}$) temperatures will be negligible and the average of both temperatures can be used as the jacket temperature. The approach is almost independent of the thermal properties and flow rate changes of jacket fluid, and thus the heat losses through the jacket have little effect on the measurement quality. However, the major problem is the estimation of the UA variations during the reaction. For instance, the reaction medium viscosity and temperature, the stirrer speed, the jacket temperature, and the flow rate of jacket fluid can all change and affect the overall heat transfer coefficient. In the case of a semi-batch operation or because of the stirrer effect, the heat transfer area can also vary. Thus determination of UA variations during the reaction is a difficult task. However, there are a few procedures used in commercial calorimeters to overcome UA determination. In RC1 (Metler Toledo AG, Switzerland) and Simular (HEL Ltd., UK), a calibration procedure is carried out before and after the experiment using a variable power electrical heater inserted inside the reactor. A known power is continuously added to the reactor medium. At the steady state and equilibrium condition, the measured temperatures and the known heater power input (q_{cal}) are used to estimate UA before and after the reaction. An assumed profile between the static values of UA at the beginning and end of the experiment is used to interpolate the UA values during the reaction. Linear interpolation of the feeding profile or realized heat profile is the most common interpolation scheme used to estimate UA. However, all procedures fail when applied to large or non-linear variations of UA. The majority of polymerization reactions, crystallization processes as well as biochemical reactions show large variations in UA. A superior approach is to evaluate UA continuously during the experiment. Inducing sinusoidal temperature oscillations by an electrical heater in the reactor or in the jacket and applying a mathematical computation procedure provide a reliable method for the estimation of the overall heat transfer coefficient [15, 28, 29]. In another approach, the convective heat transfer coefficients on the reactor and jacket sides can be measured before the onset of the reaction [13].

Heat balance calorimetry

The same procedure mentioned for heat flow calorimetry is used to control the reactor temperature in the heat balance calorimetry. However the measurement and calculation procedures are totally different and depend completely on the jacket system. The calculation of heat exchange between the reactor medium and the jacket fluid is independent of UA value and is based on the sensible energy changes of the jacket fluid.

$$q_{ex}=m_j^0 c_{p,j}(T_{j,out}-T_{j,in}) \quad (4)$$

where m_j^0 and $c_{p,j}$ are mass flow rate and specific heat capacity of the jacket fluid, respectively. In this case, also a high flow rate for the jacket fluid is needed to control the reaction temperature perfectly. Thus the difference between the outlet and inlet jacket temperature is relatively small. High precision measurements of the flow rate and temperatures are required to calculate accurately the rate of heat exchange using

Eq. (4). Compared to heat flow calorimetry, this method has lower sensitivity. Small heat losses to the surroundings through the jacket wall introduce significant errors in heat calculation and thus perfect insulation is required.

Heat compensation calorimetry

The jacket temperature is artificially adjusted a few degree (e.g. 20°C) lower than the desired reactor temperature. Manipulation of the power of a precise heater inserted inside the reactor ensures the control of the reactor temperature. A constant temperature difference between the reactor and jacket temperature is achieved using the compensated power, which will be constant at steady state. Thus, the process thermal effects can be directly inferred from the compensation heater power input. Neither calibration nor temperature measurement, in contrast to heat flow and heat balance calorimetry, is required for the heat calculations. The technique is independent of *UA* variations as well as jacket media properties. Because of large response time, this method is recommended for fast reactions. However, in the crystallization systems, the fine particles may dissolve close to the hot spots of the heater surface. Due to fouling on the heater surface, the method is not recommended for the viscose and heat sensitive systems. Also, to determine correctly the heat flow rate, a baseline correction is needed if the *UA* varies during the process [30]. Available commercial calorimeters based on heat compensation technique are Simular (HEL Ltd., UK) and AutoMate [31].

Peltier calorimetry

A similar setup is used for the Peltier calorimeter. However the reactor wall, except the bottom, is thermally isolated from the jacket side and the heat transfer area is limited to the bottom surface. A Peltier element mounted on the reactor bottom is used for both cooling and heating purposes. In Peltier calorimeter, the jacket temperature is adjusted at a constant temperature and the reactor temperature is controlled by manipulating the Peltier element power. Combination of the measured power and heat balance theory is used for the calorimetric calculations. The approach is independent of reaction media and heat transfer area variations. However, because of heat transfer area limitations, the *UA* variations cannot be inferred for the scale-up purposes. Also a pre-calibration is needed for Peltier element. The CPA200 (ChemiSens AB, Sweden) is one of the commercial reaction calorimeters designed and built on Peltier calorimetric principle.

To overcome some of the disadvantages of the methods currently used in the commercial calorimeters, we propose heat flux sensors to measure q_{ex}, directly. The proposed technique is based on heat flow calorimetry; however, a new approach is used to measure heat flow rate through the reactor wall. Although a calibration procedure before or after the reaction to evaluate the lateral heat transfer area is needed in the proposed technique, it is independent of reaction media and the overall heat transfer coefficient can be inferred during the reaction.

Experimental

All experiments were carried out in a 2.5-L (*ID*=14.0 cm; *h*=16.9 cm) stainless-steel triple-jacketed reactor as shown in Fig. 1. The outer jacket was vacuumed and used to thermally insulate the reactor. The vessel was fitted with a variable speed stirrer (anchor type with 6.0-cm diameter, 8.0-cm height and 0.9-cm blade width) 3.0 cm above the reactor bottom for gentle mixing, a variable power heater for calibration procedure before or after the reaction, and a feed pump. Because of possibility of sensor damage due to erosion or corrosion, four sensitive and precise 5.1×5.1 cm heat flux sensors (flexible-small bend radius BF heat flux transducer, Vatell Corporation, VA, USA) were mounted on the outside wall of the reactor. Two thermopile junction layers separated by a thin layer of thermal resistance material were used to construct the sensors with maximum temperature and response time of 170°C and 0.9 s, respectively. Introducing a heat flow across the thermal resistance produces a temperature gradient between each thermocouple pair of the thermopile and registers a differential voltage, which is proportional to the heat flux. The magnitude and the direction of the heat flux can be inferred from the sum of the differential voltages. The heat transfer properties of the lateral and bottom areas of the reactor are totally different. Thus

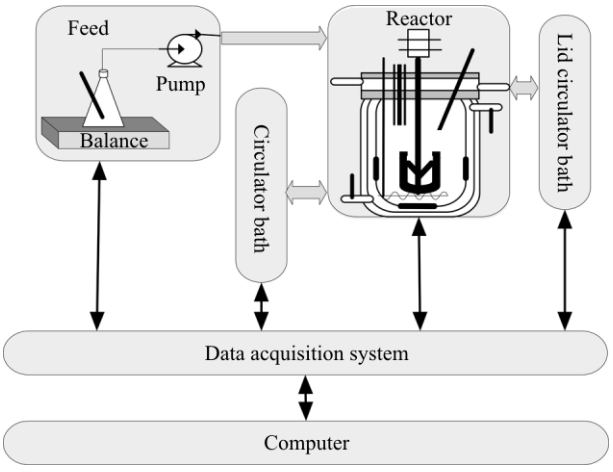

Fig. 1 Experimental setup

three sensors were mounted symmetrically on the lateral surface (2 cm above the reactor bottom) and another one on the center of the reactor bottom. Before mounting the transducers, the reactor wall and sensor surfaces were cleaned and dried. A thin and uniform layer of a paste (OT-201, Omega, CT, USA) with high thermal conductivity (2.3 W m^{-1} K^{-1}) was applied to both surfaces. The transducers were mounted using a high thermal conductive (1.4 W m^{-1} K^{-1}) epoxy adhesive (OB-200, Omega, CT, USA). Care was taken to ensure that no bubbles were trapped between the two surfaces. The voltage output of the transducers was measured precisely (0.01 mV) and then converted to the heat flux (W cm^{-2}) using sensors' calibration values (in mV W^{-1} cm^{-2}) presented by Vatell Corporation (linear calibration curve). The average of three lateral sensor outputs and the bottom sensor output were used to calculate the heat exchange between the reactor content and jacket fluid. Also the temperature of outer surface of the reactor was measured locally using each transducer equipped with a separate thermocouple.

The solution temperature measured by an RTD probe (Omega, CT, USA) with 0.1°C resolution was varied by manipulating the temperature of the cooling water through the jacket. Manipulation of the cooling water temperature was achieved by adjusting the set point of a water bath system (FP-50, Julabo Labortechnik GMB H, Germany) through a three-level cascade control system. The reactor lid was jacketed and a separate thermostatically controlled bath (F-30, Julabo Labortechnik GMB H, Germany) was used to circulate water through the reactor lid to keep its temperature a few degrees above the reaction temperature for preventing heat losses from the lid. In semi-batch experiments, a balance (0.01 g precision, Ohaus, NJ, USA) and a variable flow rate pump (QVG50, Fluid metering INC., NY, USA) were used to measure and to control the flow rate of the reactant, respectively. The temperatures of the feed, jacket input and output streams were measured using three RTD probes (0.1°C resolution), pre-calibrated by a thermometer with a resolution of 0.1°C. LabView (National Instruments, TX, USA) hardware/software module was used for data acquisition and control with a sampling time of 0.5 s and a data saving frequency of 10 s.

Experiments were performed to test the new calorimetric system and to show its capability and precision. Acetic anhydride (99.4–99.7%, Fisher Scientific, New Jersey, USA), Glycerin (99.9%, Fisher Scientific, New Jersey, USA), and deionized water were used in this study.

Determination of sensitivity and relative detection limit

To determine the power detection limit relative to the sample volume (W L^{-1}) [30], the reactor was charged with 2 kg of water and the constant jacket temperature method (isoperibolic mode) was used. The temperatures of the jacket and lid water circulating baths were set at 20 and 22°C, respectively. The heater input power was set at 2.0, 3.8, 7.5, 15.0, 30.0 and 45.0 W. At each heater power input, the attainment of steady state was confirmed by the heat flux readings. The water level inside the reactor was calculated using the measured liquid level at the onset of the experiment and the volume of the internals. The heat input at each steady state level was then calculated using the baseline data for the heat losses and the stirring power, predicted lateral area, as well as the bottom area and compared with the actual heat input. The procedure was repeated for the constant jacket temperature of 25 and 30°C.

Hydrolysis of acetic anhydride in a semi-batch reactor

To validate the performance of the proposed calorimetric technique, hydrolysis of acetic anhydride is used as a model reaction. The reaction is exothermic and second order with respect to acetic anhydride (A) and water, however it can be considered as a pseudo-first-order reaction in the presence of excess water [27, 32]. Assuming constant feed molar flow rate ($F_{A,f}$) for an isothermal first-order reaction with zero initial condition, the number of moles of A in the reactor (N_A) as a function of real time (t), can be derived [33] for the semi-batch operation.

$$N_A = \frac{F_{A,f}}{k}(1-e^{-kt}) \tag{5}$$

where k is reaction rate constant. Using a mole balance for reactant A, the N_A can be related to the conversion of the reaction (X); the moles of A reacted per mole of A fed to the reactor.

$$N_A = N_{A,0} + F_{A,f}t - N_{A,t}X \tag{6}$$

where $N_{A,t}$ and $N_{A,0}$ are the total number of moles A fed to the reactor and the number of moles A in the reactor initially, respectively. Substituting Eq. (5) into Eq. (6) and rearranging yields.

$$X = \frac{F_{A,f}}{N_{A,t}}\left(t - \frac{1-e^{-kt}}{k}\right) \tag{7}$$

If the same approach is applied to the batch reactor, the batch conversion (X_b) can be obtained as a function of batch time (t_b).

$$X_b = 1-e^{-kt_b} \tag{8}$$

where X_b is defined as the moles of A reacted per mole of A charged initially to the reactor.

If the reaction goes to completion with A as the limiting reactant, the total heat generated by the reaction (Q_t) will be expressed as:

$$Q_t = N_{A,t}(-\Delta H_{r,T}) \quad (9)$$

At time t, the ratio of total power measured by the calorimetric technique to Q_t represents the thermal conversion (X_{th}).

$$X_{th} = \frac{\int_0^t q_r \mathrm{d}t}{Q_t} \quad (10)$$

where $\Delta H_{r,T}$ is the molar enthalpy of the reaction at the reactor working temperature T. Because of availability of data in the literatures, hydrolysis of acetic anhydride was carried out at 25°C.

A known quantity of water was initially added to the reactor and the stirrer was turned on. Using the constant jacket temperature mode, the jacket and lid temperatures were set at 25 and 27°C, respectively. The system was run to achieve the first steady state as a baseline for the calibration procedure before the onset of the experiment. The heater was then adjusted to 45-W power until the second steady state was observed. After scanning almost 20 data points at the steady state, the power was turned off and the system was switched to the isothermal mode. The next observed steady state level was used as the reaction baseline and the acetic anhydride pump was started at constant flow rate. To follow the concentration profile of acetic anhydride, FTIR spectra of the solution in the wavenumber range 850–1750 cm^{-1} was also taken during the reaction. When the reactant was completely charged, the second calibration was initiated. This experiment was carried out four times (R1–R4) at different conditions.

A simulated reaction with viscosity variations

This set of experiments was designed to test the U variations. A mixture of glycerin and water, at different concentration was used to investigate the effect of variations in U. One and ninety one hundredth kilogram of diluted glycerin (94% mass basis) was initially charged to the reactor. For gentle and homogeneous mixing, an additional anchor stirrer (with 13.0-cm diameter, 8.7-cm height, and 0.9-cm blade width) was coupled to the first one with 90° angle and fitted 3 cm above the reactor bottom. The speed was adjusted at 200 rpm. The heater was inserted in the space between the two stirrers. The reactor and lid temperatures were set at 20 and 22°C, respectively. After reaching the first steady state and scanning some data for the baseline, the heater was set at 30 W as the source of generated energy. First, the system was run to adjust the reactor temperature at 20°C. Then the water was pumped into the reactor at constant flow rate, 4.61 g min^{-1}. Four hundred and eighty-four gram of water was added to change the glycerin mass percent to 75. Then both the pump and the heater were turned off and the system was switched to isoperibolic mode. When the system showed the second steady state condition, 41 g of water at 20°C was added into the reactor in one min to estimate the heat of mixing. The system was run until the third steady state was reached. Then, the calibration procedure was carried out to evaluate the lateral area. Also the viscosity of the 94 and 75% glycerin solutions at 20°C was measured using an off-line viscometer (DV-E, Brookfield, MA, USA).

Results and discussion

Detection limit

Figures 2a and b show the temperature changes (reactor, jacket, reactor lateral wall and reactor bottom) and the heat flux outputs (reactor bottom and lateral wall average) for detection limit runs at constant jacket temperature 20°C. For each step of adding a known heat power to the system, the temperatures, except the jacket temperature, increase from a steady state level to a new level. The outputs of the heat flux sensors follow the same trend. As expected, the heat flux through the reactor bottom is lower than that through the lateral wall.

In order to evaluate the accuracy of the proposed system, the actual power input to the reactor and the

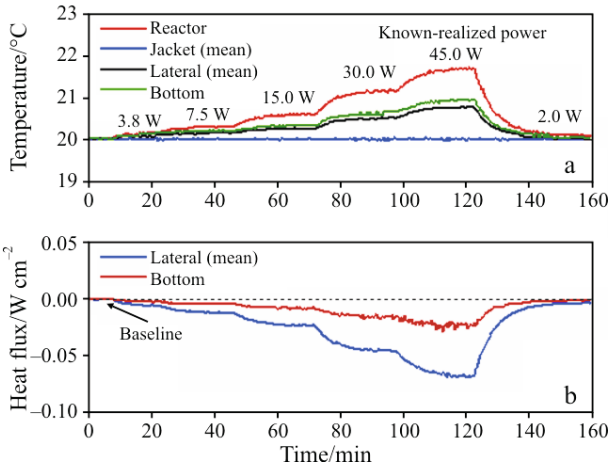

Fig. 2 Evaluation of relative detection limit using different heater power inputs at constant jacket temperature 20°C; a – reactor, average jacket, reactor bottom and reactor lateral wall temperatures; b – heat flux through the reactor bottom and lateral wall

Table 1 Predicted water level, measured and predicted heat input by the heater and overall heat transfer coefficients for different constant jacket temperatures

Jacket temp./°C	Water level/cm		Measured (M) and predicted (P) heat input by the heater at steady state intervals (t)														Overall heat transfer coefficient/W m^{-2} $°C^{-1}$	
	Measured	Predicted by 45-W run	2.0-W run			3.8-W run			7.5-W run			15.0-W run			30.0-W run			15.0-W run	30.0-W run
			t/ s	*M*/ kJ	*P*/ kJ	*t*/ s	*M*/ kJ	*P*/ kJ	*t*/ s	*M*/ kJ	*P*/ kJ	*t*/ s	*M*/ kJ	*P*/ kJ	*t*/ s	*M*/ kJ	*P*/ kJ		
20	12.1	11.3	380	1.00	0.76	360	1.23	1.37	510	3.77	3.83	410	6.21	6.15	250	7.52	7.50	313.3	319.2
25	12.0	11.3	400	0.87	0.80	380	1.52	1.44	500	3.81	3.75	430	6.44	6.45	280	8.20	8.40	324.7	325.7
30	12.0	11.3	440	0.85	0.88	420	1.66	1.60	430	3.17	3.23	450	6.94	6.75	250	7.67	7.50	330.3	335.9

calculated power are compared at each steady level. The latter is evaluated using the outputs of the heat flux sensors and Eq. (2). The rate of stirrer power input is a function of the stirrer speed and solution viscosity represented by the torque. The stirring power is usually taken into account by measuring the torque and the stirrer speed [16, 18]. Also the heat losses from the reactor is considered proportional to the temperature difference between reactor and ambient temperature [11, 16, 18, 26, 30] or is calculated as being proportional to the total vapor pressure of reactor content [6, 7]. In the present approach, however, the heat losses and the stirrer power input can be inferred using the baseline outputs of lateral heat flux ($Q^{*,l}_{ex,B}$) and bottom heat flux ($Q^{*,b}_{ex,B}$) sensors (in W cm^{-2}). For the baseline condition, the Eq. (2) is simplified to:

$$(q_s - q_l) = q_{ex} = A^l Q^{*,l}_{ex,B} + A^b Q^{*,b}_{ex,B} \qquad (11)$$

where A^l and A^b are the lateral and bottom heat transfer surfaces, respectively. To do the calculations, the heat transfer area has to be known. The bottom area is constant and known; however, the lateral area varies with the level of water inside the reactor. In order to calculate the latter, the steady state data from the 45-W heater is applied to Eq. (2). In this case (steady state with no feed and no reaction) q_f, q_{hm} and q_r are zero. Thus

$$q_h - q_{ex} + (q_s - q_l) = 0$$

or

$$q_h - [A^l Q^{*,l}_{ex} + A^b Q^{*,b}_{ex}] + (q_s - q_l) =$$
$$q_h - [A^l (Q^{*,l}_{ex} - Q^{*,l}_{ex,B}) + A^b (Q^{*,b}_{ex} - Q^{*,b}_{ex,B})] = 0 \qquad (12)$$

Because all terms in Eq. (12), except A^l, are known, the lateral heat transfer surface can be calculated. The other heater power inputs are evaluated at their steady level using Eq. (12), the predicted lateral, the known bottom surface and the heat flux sensor outputs (the results were in W and then were converted to kJ using the corresponding interval time at each steady state level). The same procedure is applied for constant jacket temperature 25 and 30°C runs and then the results are summarized in Table 1. For all runs, the predicted water level is compared well with the measured water level, 11.3 cm. The difference is attributed to the stirrer effect. Also predicted heater power inputs are in good agreement with the actual power inputs.

The overall heat transfer coefficient is also evaluated using Eq. (3). The calculated values for 15 and 30-W runs are listed in Table 1. Because of different working temperatures, small changes in the U are observed. In fact, at the same fluid flow condition, increasing the reactor and jacket temperatures results in a small increase in the overall heat transfer coefficient, which is consistent with the heat transfer theory.

The relative detection limit was determined using the lowest power input, 2 W, in the range of 0.8–1 W L^{-1}. This limit is comparable with the relative detection limit of standard reaction calorimeters reported in the literatures [30].

Hydrolysis of acetic anhydride

For a typical experiment, the variations of reactor and jacket temperatures as well as the lateral and bottom heat fluxes are sketched in Figs. 3a and b, respectively. Using Eq. (12) and the corresponding baseline information, the data obtained from the first and second calibrations are applied to estimate the lateral area before and after the reaction, respectively. The calculations indicate a lateral area of 606.5 cm^2 at the end of the reaction. Deducting the increased area due to 205 g of added acetic anhydride results in 547.1 cm^2 for the lateral area at the onset of the reaction. This area was estimated as 547.8 cm^2 using the first calibration. The results show that both calibrations at the onset and end of reaction agree well.

During the reaction, the reactor temperature remains constant after a small deviation (≈0.3°C) from the set point at the beginning. The deviation is also observed at the end of experiment after stopping the feed. The deviations are due to the control system and are low enough to be ignored. Comparing the FTIR spectra of pure water, acetic acid, and acetic anhydride in the wavenumber range 850–1750 cm^{-1}, indicates that the peak in the range 1100–1200 cm^{-1} is a good representation of the acetic anhydride concentration (water and acetic anhydride have no IR peaks in this range). In spite of plotting the spectra in the whole range, the FTIR spectra of the solution taken at

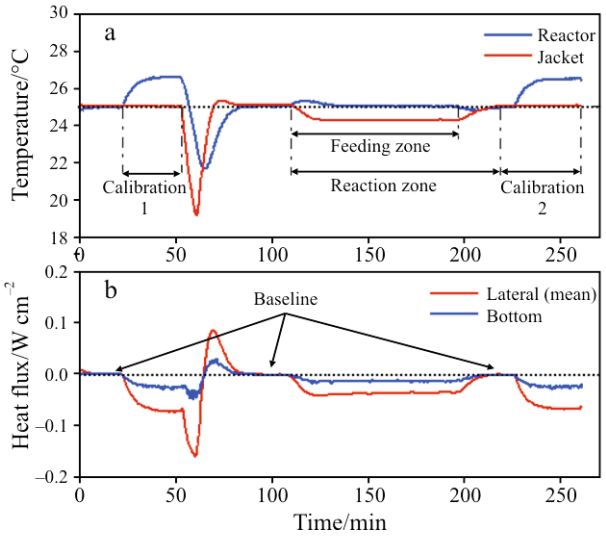

Fig. 3 Variations in a – temperature and b – heat flux profiles for hydrolysis of acetic anhydride at constant feed flow rate and 25°C (run R1)

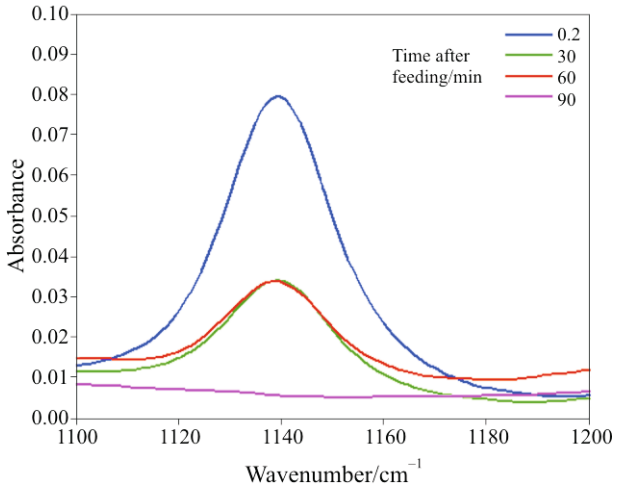

Fig. 4 FTIR spectra of the solution during hydrolysis reaction of acetic anhydride for experiment R1

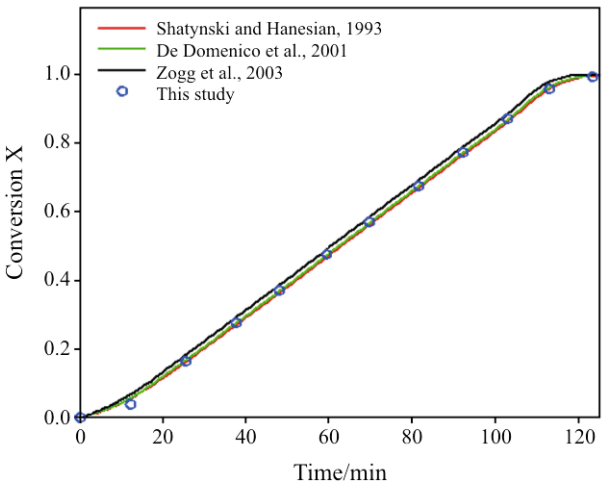

Fig. 5 Conversion of hydrolysis of acetic anhydride *vs*. time for semi-batch experiment R2 at 25°C

the beginning of reaction, during the reaction, and one min after stopping the feed are sketched in Fig. 4 for the range 1100–1200 cm^{-1}. At the beginning, the concentration is relatively high, however, it remains constant at lower level during feeding (with constant flow rate) and becomes zero only one min after stopping the feed. Thus it can be inferred that the reaction is fast enough to calculate the heat of reaction during the isothermal profile only.

Twenty scanned data points were chosen for the calculation. The exchanged heat is evaluated using the outputs of heat flux sensors, the predicted lateral area, and the bottom area. The results are corrected based on the baselines before and after the reaction for the heat losses and the stirring power. The heat of dosing is calculated using the measured feed flow rate (m_f^0), feed temperature (T_f) and reactor temperature.

$$q_f = \sum m_f^0 c_{p,f} (T_f - T_r) \qquad (13)$$

where $c_{p,f}$, is specific heat capacity of the reactant (s).

These values provide enough data to apply Eq. (2) for estimation of heat of reaction including heat of mixing at each interval. The average of obtained results from all intervals is then used for the final value. The results together with experimental conditions for four runs (R1–R4) are listed in Table 2. The estimated heats of reaction show –62.5±0.7 kJ mol^{-1} for the mean value at 25°C. The result is in very good agreement with the range (57–64 kJ mol^{-1}) of heat of reaction (including heat of mixing) reported in literatures [3, 31].

The conversion of the reaction estimated from Eq. (10) was compared with the corresponding values reported in the literatures [3, 27, 32]. The conversion was calculated using the k values and Eq. (7). Equation (8) was used after stopping the feed (batch-wise operation). The results of R2 experiment are plotted in Fig. 5. The excellent match is an indication of the validity of our approach. It is noted that the k value reported by Zogg *et al.* [27] was obtained under catalyzed condition (H^+) showing higher reaction rate for hydrolysis of acetic anhydride. Thus the small difference in conversion can be attributed to the different reaction conditions used.

The overall heat transfer coefficient was also evaluated at each interval during the isothermal condition. The temperature difference between the reactor content and the jacket fluid is almost constant and the heat flux sensors show almost constant values during the reaction (Fig. 3). Therefore a constant value for the overall heat transfer coefficient is expected. For experiment R2, for instance, the U values calculated using Eq. (3) are in the range 374–379 W m^{-2} C^{-1} with a mean value 376±2 W m^{-2} C^{-1}. The mean value is in the range of the

Table 2 Conditions of 4 replicate experiments for hydrolysis of acetic anhydride at 25°C

Run	Speed of stirrer/rpm	Acetic anhydride/water mole ratio	Total acetic anhydride added/g	Purity of acetic anhydride/%	Feed flow rate/g min^{-1}	ΔH_r including heat of mixing/kJ mol^{-1}
R1	150	1:50	205	99.5	2.34	–62.9
R2	120	1:40	312	99.7	2.88	–62.4
R3	180	1:55	215	99.4	3.18	–61.6
R4	220	1:38	300	99.4	2.01	–63.2

overall heat transfer coefficient (200–850 W m^{-2} C^{-1}) reported for jacketed vessels using water as the heating/cooling fluid, aqueous solution as fluid in vessel and stainless steel as the reactor wall material [34].

Estimation of thermal effects with a varying overall heat transfer coefficient

The temperature and the heat flux profiles for the water–glycerin experiments are shown in Fig. 6. Adding water to 94% glycerin solution at 20°C changes the measured viscosity from almost 610 to 40 mPa s. The viscosity changes result in the overall heat transfer coefficient variations during the process. As long as the heater power input is kept constant, the temperature difference between the reactor and the jacket decreases to compensate the U variations for an isothermal process. In order to demonstrate the capability of the proposed calorimetry in the presence of U variations, the lateral surface area is evaluated using Eq. (12), the third baseline, and the final calibration data.

Deviations of the solution temperature from the set point at the beginning of the feed addition can be attributed to the heat of mixing (the feed temperature was 20°C). Thus the accurate heat calculations need an estimation of the heat of mixing. Figure 7 shows the heat flux outputs corresponding to the heat of mixing zone. Using the data of heat flux sensors, the estimated heat of mixing is –27.5 J g^{-1} of added water. Although the value may vary at different glycerin compositions, it was used for the entire heat calculations.

The estimated lateral heat transfer was then corrected using the added water for the heat of mixing measurement. The heat of dosing is determined using Eq. (13). The heat losses and the stirrer power effects were evaluated using the baseline data as well. Equation (2) was applied to estimate the generated heat at

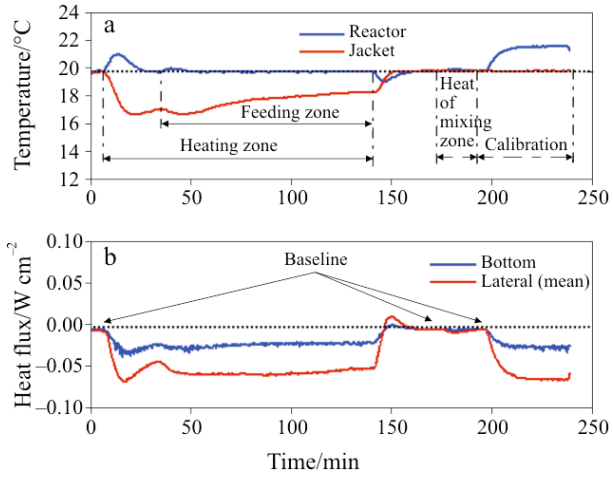

Fig. 6 Variations in a – temperature and b – heat flux profiles for simulated reaction at constant feed flow rate and 20°C

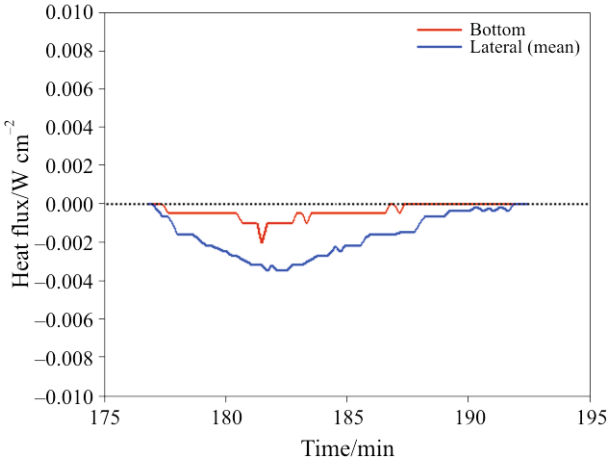

Fig. 7 Heat flux outputs at heat of mixing zone after baseline correction

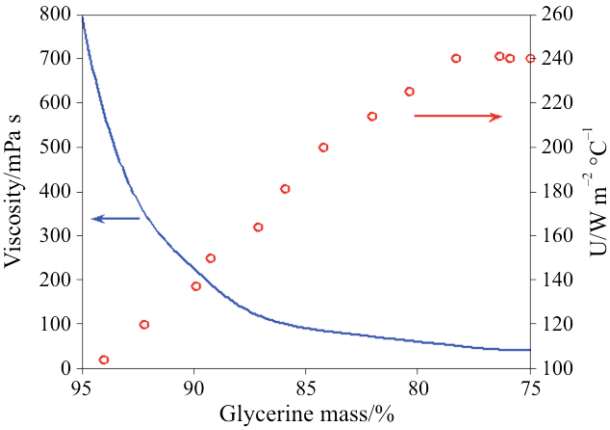

Fig. 8 Viscosity and overall heat transfer coefficient variations during the simulated reaction

each interval. The total generated heat for the entire elapsed time was –192.3 kJ (–30.5 W), which is in good agreement with the actual heater power input of –189.1 kJ (–30.0 W).

To show the effect of changes in viscosity, the overall heat transfer coefficient was determined for each interval using Eq. (3), the measured temperature difference, the corrected heat transfer area using the mass of dosing, and the estimated heat. The viscosity variations as a function of glycerin concentration at 20°C are adopted from Weast and Astle [35]. The measured viscosity for 94 and 75% glycerin solutions are in good agreement with the reported data. Both the estimated U and the viscosity variations are sketched *vs.* glycerin mass percent in Fig. 8. As the viscosity decreases sharply at the beginning of the experiment, the overall heat transfer coefficient increases rapidly. The U variations also show the same increasing trend corresponding to viscosity changes. The viscosity changes are very small when the glycerin mass percent is decreased from 80 to 75%. Thus,

within this range, U remains almost constant as expected. The results show the capability of the proposed calorimetry system to deal with the U variations.

Conclusions

A new heat calorimetry using the heat flux sensors for the isothermal-heat flow mode is developed. The results reported in this study indicate the superiority of the proposed reaction calorimetry for exothermic or endothermic reactions. The heat flux sensors are independent of the reactor content and jacket fluid and exhibit high sensitivity and accuracy in the presence of the variations in the overall heat transfer coefficient. No pre-calibration is needed for the sensors before running the experiments and no heating element is applied inside the reactor for temperature control. The method serves as a useful technique to help assess the UA variations without complicated calculations and can be applied to viscous and heat sensitive systems. The stirrer power and the heat losses from the reacting vessel can be determined easily. However, the calculations still rely on an estimation of the lateral heat transfer area using a calibration procedure before or after the reaction. Similar to the commercial reaction calorimetry techniques, the proposed method has a relatively large response time with respect to the reactor temperature control and is very sensitive to homogeneity of the reactor content. Poor mixing can lead to the variations in the heat transfer through the wall and thus an incorrect value is expected for the fixed position heat flux sensors. Future work should focus on developing easier approaches to eliminate the lateral area, improving the detection limit, and reducing the response time for the reactor temperature control.

Acknowledgements

The authors are grateful for the financial support provided by the Natural Sciences and Engineering Research Council (NSERC) of Canada and Canada Foundation for Innovation (CFI). The University of Western Ontario machineshop is gratefully acknowledged for making the reactor. Fellowship students, Hung Nguyen and Dhiraj Agrawal, are also acknowledged for their help in LabView software programming.

Notation

A	Heat transfer area (m^2)
C_p	Heat capacity (J g^{-1} °C^{-1})
F	Molar flow rate (mol s^{-1})
h	Height
ID	Inside diameter
k	First order reaction rate constant (s^{-1})
m	Mass (g)
m^0	Mass flow rate (g s^{-1})
N	Reactant moles (mol)
q_{ex}	Heat power exchanged through the reactor wall (W)
q_f	Heat power due to reactant dosing (W)
q_h	Heater power (W)
q_{hm}	Heat of mixing (W)
q_l	Heat losses (W)
q_r	Reaction power (W)
q_s	Stirrer power (W)
Q	Generated or consumed heat by the reaction (J)
Q^*_{ex}	Heat flux exchanged through the reactor wall (W cm^{-2})
t	Time (s or min)
T	Temperature (°C)
U	Overall heat transfer coefficient (W m^{-2} °C^{-1})
X	Conversion

Greek letter

$\Delta H_{r,T}$	Heat of reaction at temperature T (J mol^{-1})

Subscript

0	Initial
A	Reactant A
b	Batch
B	Baseline
f	Feed
i	i^{th} components in the reaction media
in	Input
j	Jacket
k	k^{th} equipments inserted inside the reaction
out	Output
r	Reactor
t	Total
th	Thermal

Superscript

l	Lateral
b	Bottom

References

1 Y. S. Duh, C. C. Hsu, C. S. Kao and S. W. Yu, Thermochim. Acta, 285 (1996) 67.
2 J. Pastré, A. Zogg, F. Stoessel, U. Fischer and K. Hungerbühler, Org. Proc. Res. Develop., 5 (2001) 158.
3 G. De Domenico, D. G. Lister, G. Maschio and A. Stassi, J. Them. Anal. Cal., 66 (2001) 815.
4 E. Molga and R. Cherbański, Chem. Eng. Sci., 54 (1999) 2467.
5 E. J. Molga, B. A. A. van Woezik and K. R. Westerterp, Chem. Eng. Proc., 39 (2000) 323.

6 O. Ubrich, B. Srinivasan, P. Lerena, D. Bonvin and F. Stoessel, J. Loss Prevention Process Industries, 12 (1999) 485.
7 O. Ubrich, B. Srinivasan, P. Lerena, D. Bonvin and F. Stoessel, Chem. Eng. Sci., 56 (2001) 5147.
8 K. Heldt, H. L. Anderson and B. Hinz, Thermochim. Acta, 310 (1998) 179.
9 A. Miyake, A. Kimura, T. Ogawa, Y. Satoh and M. Inano, J. Therm. Anal. Cal., 80 (2005) 515.
10 D. J. am Ende, P. J. Clifford and D. L. Northrup, Thermochim. Acta, 289 (1996) 143.
11 J. Zeaiter, V. G. Gomes, J. A. Romagnoli and G. W. Barton, Chem. Eng. J., 89 (2002) 37.
12 L. López de Arbina, L. M. Gugliotta, M .J. Barandiaran and J. M. Asua, Polymer, 39 (1998) 4047.
13 I. Sáenz de Buruaga, A. Echevarría, P. D. Armitage, J. C. de la Cal, J. R. Leiza and J. M. Asua, AICHE J., 43 (1997) 1069.
14 L. M. Gugliotta, J. R. Leiza, M. Arotçarena, P. D. Armitage and J. M. Asua, Ind. Eng. Chem. Res., 34 (1995) 3899.
15 F. Dan, M. H. Hamedi and J.-P. E. Grolier, J. Therm. Anal. Cal., 85 (2006) 531.
16 D. Voisard, U. von Stockar and I. W. Marison, Thermochim. Acta, 394 (2002) 99.
17 F. Aulenta, C. Bassani, J. Ligthart, M. Majone and A. Tilche, Water Res., 36 (2002) 1297.
18 M. C. García-Payo, S. Ampuero, J. S. Liu, I. W. Marison and U. von Stockar, Thermochim. Acta, 391 (2002) 25.
19 H. Graebner, R. Kirchner, J. Lerchner and G. Wolf, Thermochim. Acta, 337 (1999) 39.
20 P. G. Royall and S. Gaisford, Curr. Pharmaceutical Biotechnol., 6 (2005) 1.
21 S. Yang and A. Navrotsky, Microporous Mesoporous Mater., 52 (2002) 93.
22 O. Söhnel, M. Kroupa, G. Franková and V. Velich, Thermochim. Acta, 306 (1997) 7.
23 O. Monnier, G. Févotte, C. Hoff and J. P. Klein, Chem. Eng. Sci., 52 (1997) 1125.
24 G. Févotte and J. P. Klein, Chem. Eng. J., 59 (1995) 143.
25 W. Hemminger and G. Höhne, Calorimetry, Fundamentals and Practice, Verlag Chemie, Germany 1984.
26 M. Schlegel and A. Löwe, Chem. Eng. Process, 37 (1998) 61.
27 A. Zogg, U. Fischer and K. Hungerbühler, Ind. Eng. Chem. Res., 42 (2003) 767.
28 L. Bou-Diab, B. Schenker, I. Marison, S. Ampuero and U. von Stockar, Chem. Eng. J., 81 (2001) 113.
29 R. Carloff, A. Proß and K. H. Reichert, Chem. Eng. Technol., 17 (1994) 406.
30 A. Zogg, F. Stoessel, U. Fischer and K. Hungerbühler, Thermochim. Acta, 419 (2004) 1.
31 C. Simms and J. Singh, Org. Proc. Res. Develop., 4 (2000) 554.
32 J. J. Shatynaski and D. Hanesian, Ind. Eng. Chem. Res., 32 (1993) 594.
33 H. S. Fogler, Elements of Chemical Reaction Engineering, Prentice-Hall, New Jersey 1986, pp. 144–147.
34 R. H. Perry and D. W. Green, Perry's Chemical Engineer's Handbook, 7th Ed., McGraw–Hill, USA 1997, p. 11.27.
35 R. C. Weast and M. J. Astle, CRC Handbook of Chemistry and Physics, 60th Ed., CRC Press, USA 1980, pp. D239–240.

Received: April 7, 2008
Accepted: July 8, 2008
OnlineFirst: November 12, 2008

DOI: 10.1007/s10973-008-9165-1